

doi:10.3788/gzxb20144310.1010005

基于边缘强度相似性的干扰图像尺度分析

吴云龙, 孙晓泉, 闫飞, 邵立, 徐银

(脉冲功率激光技术国家重点实验室, 合肥 230037)

摘要:为了客观、准确及定量地评估激光干扰效果,给出了图像边缘强度的定义及计算方法,提出了一种基于边缘强度相似度的干扰图像尺度。该尺度通过计算目标图像和背景图像的相似程度来衡量激光干扰效果,相似度越高表明激光干扰效果越好。激光视场内及视场外干扰实验与数值计算表明:该图像尺度可以较好反映激光干扰对 CCD 成像探测系统目标检测算法性能的影响。同时,通过对荷兰 TNO 研究所提出的 Search_2 数据库的计算表明,提出的干扰图像尺度和目前常用光电图像杂波尺度相比,与实际人眼实验结果具有更好的一致性。

关键词:激光干扰;成像系统;边缘强度;效果评估;Search_2 数据库

中图分类号:TN977

文献标识码:A

文章编号:1004-4213(2014)10-1010005-6

Image Metrics Analysis of Laser Interference Effect Based on Edge Strength Similarity

WU Yun-long, SUN Xiao-quan, YAN Fei, SHAO Li, XU Yin

(State Key Laboratory of Pulsed Power Laser Technology, Hefei 230037, China)

Abstract: In order to evaluate the performance of laser jamming objectively, precisely and quantitatively, the definition of image edge strength and its computation method are provided, and an objective image metrics based on the edge strength similarity was proposed. The metrics evaluate the laser jamming performance by computing the similarity between the target image and laser jamming image. The higher the similarity between target and background is, the better the laser interference performance is. Experimental results of laser interference in and out the field of view show that the proposed metrics could realize quantitative appraisal of laser jamming performance on CCD imaging detection system and have a better consistency with the eye's experimental data in the prediction of detection probability than common clutter metrics by taking use of the Search_2 dataset.

Key words: Laser interference; Imaging system; Edge strength; Performance appraisal; Search_2 dataset

OCIS Codes: 100.2000, 100.2960, 040.1880, 110.2970

0 Introduction

In (Electro-Optics, EO) surveillance and reconnaissance imaging systems, CCD detectors are widely used for its compact size, low cost, high distinguishability, etc. Meanwhile, CCD can be interfered and damaged easily by laser when it is on

work, which could have some direct influence on the performance of CCD imaging detection system. Therefore, the study on the impact of laser radiation on CCD detection system and assessing the jamming performance legitimately and quantificationally is a significant and challenging job, which could be applied in many fields such as laser induced damage on EO

Foundation item: State Key Laboratory of Pulsed Power Laser Technology Funds (No. 13J1003); The Key Laboratory Funds of Optoelectronic Information Control and Security Technology of China (No. 20100713-003)

First author: WU Yun-long(1988-), male, master degree, mainly focuses on the assessment of laser interference performance. Email: jackwu1225@126.com

Responsible author: SUN Xiao-quan(1962-), male, professor, Ph. D. degree, mainly focuses on the optical technology. Email: sunxq@ustc.com

Received: Dec. 30, 2013; **Accepted:** Mar. 10, 2014

<http://www.photon.ac.cn>

imaging systems, optoelectronic defense technology, etc. It is known that the final information imaging detectors delivers to the observers or automatic imaging systems are images. So, making use of the images collected from imaging system could be a convenient and effective way to evaluate the performance of laser jamming on EO imaging detection systems. In the past few decades, large plenty of attention has been attracted on the research of developing objective Image Quality Assessment (IQA) metrics. Hence, more and more efficient and promising IQA metrics have been raised. However, few efforts have been conducted to verify the validity of applying such metrics into the research of laser interference performance assessment. Xu et al. proposed an integrated metrics combined with Structural Similarity Metrics (SSIM)^[1] and Root Sum of Squares metrics (RSS)^[2] to evaluate laser jamming performance on CCD imaging detection systems^[3]. Nevertheless, the comprehensive metrics can't avoid the inherent drawbacks of SSIM or RSS, e. g., they would acquire poor performance when used in complex EO scenes.

According to the mechanism of Human Visual System (HVS), human eyes are very sensitive to the edges of objects and the target with rich edge information in an image would attract more attention in general when people see it. In normal conditions, the targets that we are interested in are artificial objects and contain rich information of details^[4]. On the other hand, the laser interference will obscure the images taken from detectors and reduce the edge information of targets in them, which will make the target become similar to its background for people's eyes. When the laser interference becomes more serious, the target in the image loses more edge information and presents more similarity to its background. So, it's a feasible method to evaluate the performance of laser interference by measuring the edge strength similarity between the target and its background in laser interference images.

In this paper, we put forward a universal image metrics to assess laser interference performance, in which the edge strength of each pixel in target image is calculated to weigh its similarity to background laser jamming images. The proposed metrics could reveal the influence of laser jamming on CCD imaging detection algorithms properly correlates well with the visual characteristic.

1 Image metrics based on edge strength similarity

1.1 The definition of edge strength

The definition of edge is varying in different

occasions. Normally, the edge is a stream of pixels, at which the image alters sharply or has discontinuity^[5]. In a target acquisition procedure of EO imaging systems, the edge of an object would deliver significant semantic information to observers^[6]. The edge information in diverse directions consists of the structural characteristics of an object we are interested in. The characteristics of edge and the definition of edge strength are shown as Fig. 1.

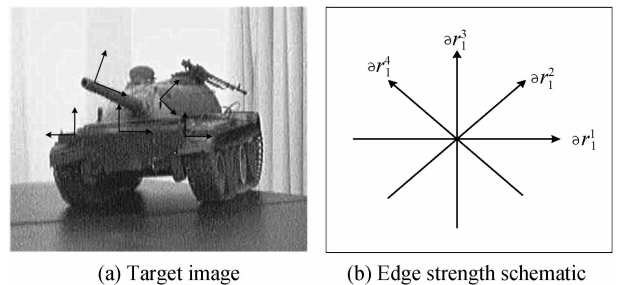


Fig. 1 The definition of edge strength

In Fig. 1 (a) the regularity of the edge along one direction, and the irregularity of the edge along the orthogonal direction. In Fig. 1 (b) the directional derivatives represent the edge strength along certain direction.

Zhang *et al.* proposed a new approach to calculate the edge strength of images^[5], motivated by its success, the definition of edge strength in this paper is based on it. Then, the edge strength of horizontal and vertical directions are defined as

$$E_i^{1,3}(r) = |\partial r_i^1 - \partial r_i^3|^C \quad (1)$$

where i represents the i th pixel in the image, $i=1, 2, \dots, N$, and N represents the total pixel numbers of the image. ∂r_i^1 represents the directional derivative along the direction 1 at the i th pixel, and ∂r_i^3 represents the directional derivative along the direction 3 at the i th pixel, which is shown in Fig. 1(b). The parameter C is a constant, which can be determined experimentally. Eq. (1) was calculated with $C=0.25m$, where $m=-10, \dots, -2, -1, 0, 1, 2, \dots, 10$ ^[5]. Similarly, the edge strength of diagonal directions are defined as

$$E_i^{2,4}(r) = |\partial r_i^2 - \partial r_i^4|^C \quad (2)$$

The total edge strength of pixel in the image could be calculated as

$$E(r, i) = \alpha E_i^{1,3}(r) + \beta E_i^{2,4}(r) \quad (3)$$

where α and β are the weights of edge strength in different directions and can be calculated by normalization method.

1.2 The ESM image metrics

With the definition of edge strength mentioned above, we can describe the concrete steps to calculate the newly proposed metrics ESM as follows in detail

1) Transform the laser jamming images acquired through CCD imaging system from RGB space to gray

space.

2) Extract target section from the jamming images manually and store the target image whose horizontal and vertical size twice of target section.

3) Divide the whole jamming image into N blocks, whose size is same with target image.

4) Compute the edge strength of target image, which could be denoted as the Eq. (3). In addition, the directional derivatives of each direction could be acquired through convolving the image with kernels, which is denoted as

$$\partial r_i^j = r * K^j, j=1,2,3,4 \quad (4)$$

the symbol $*$ in denotes two-dimensional convolution, and the kernels K^j are modelled on the basis of Scharr operator, which could be acquired in Ref. [2].

5) Calculate the edge strength of each block in the jamming image as follows

$$E_j(b, i) = \xi E_i^{1,3}(r) + \eta E_i^{2,4}(r) \quad (5)$$

where j represents the j th block in the jamming image, and i represents the i th pixel in the j th block. ξ and η are the weights of edge strength in different directions, which can be calculated by normalization method. Then, the whole edge strength vector of the image is acquired as

$$\mathbf{E}(b, i) = (E_1(b, i), E_2(b, i), \dots, E_N(b, i))^T \quad (6)$$

6) ESM of the j th block is given as follows

$$\text{ESM}_j = \| E(r, i) - E_j(b, i) \|_2 \quad (7)$$

where $\| \cdot \|_2$ represents the L_2 norm, and $E(r, i)$ is the edge strength of i th pixel in the target image.

7) The global ESM metrics could be expressed as

$$\text{ESM} = \sum_{k=1}^N t_k \cdot \text{ESM}_k \quad (8)$$

t_k is the weight for ESM_j in the vector $(\text{ESM}_1, \text{ESM}_2, \dots, \text{ESM}_j, \dots, \text{ESM}_N)$ and can be calculated by normalization method.

2 Experimental results

2.1 Performance verification

Instead of using the publically universal databases, we take actual experiments to verify the validity of proposed ESM metrics. The experimental facility we design is shown as Fig. 2.

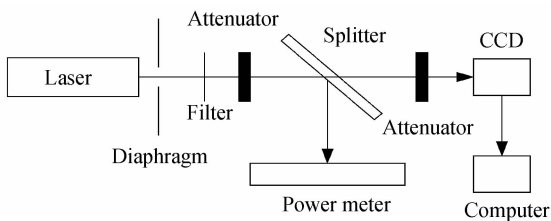


Fig. 2 Experimental facility of laser interfering CCD

The laser jamming images collected from CCD imaging systems are shown in Fig. 3 and Fig. 4, respectively.

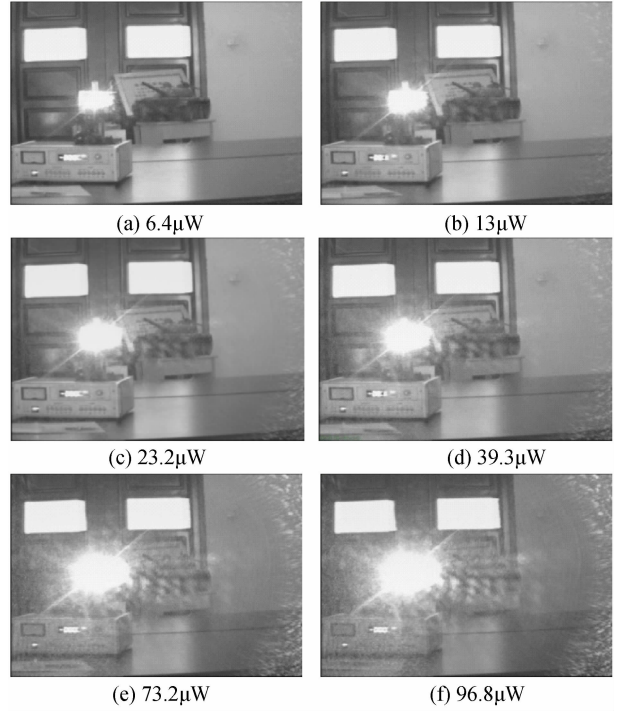


Fig. 3 Laser jamming images in the field of view

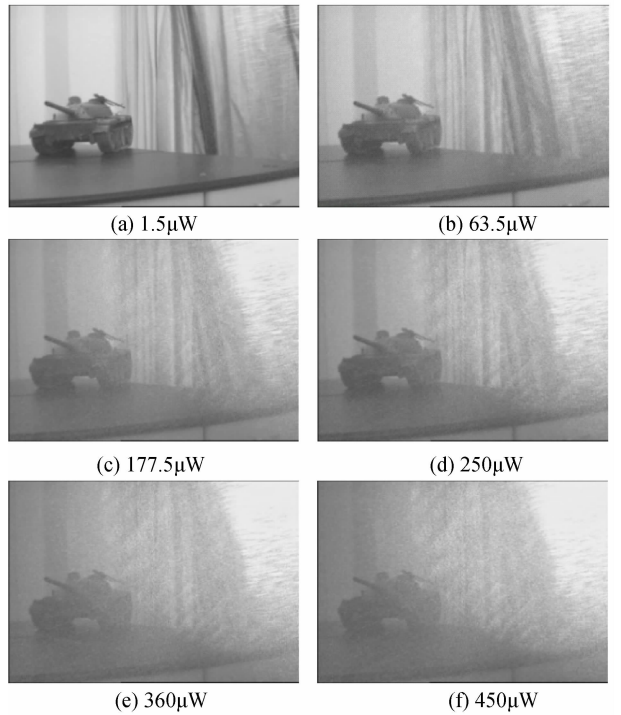


Fig. 4 Laser jamming images out the field of view

The imaging detection algorithms will be influenced mostly when laser irradiates the CCD imaging systems. Among them, Otsu segmentation algorithm and correlation detection algorithm are most widely used. Therefore, we take advantage of Otsu algorithm to compute segmentation accuracy^[9] and normalized cross correlation detection algorithm to compute false alarm probability^[10] for analysis. Then, we can acquire the numerical results corresponding to each jamming image in Fig. 3 and Fig. 4, which are

shown as Table 1 and Table 2. The parameter SA in tables denotes segmentation accuracy and P_{fa} denotes false alarm probability.

What's should be noted especially is that we set parameter C as different values for two separate situations, namely, C equals 2 when the incident laser power is relatively low and C equals 0.5 when the incident laser power is relatively high. In this study, set C as 2 for incident laser in the field of view and C as 0.5 for incident laser out the field of view.

It is shown in Table 1 that the segmentation accuracy of Otsu algorithm decreases monotonously along with incident laser power increasing, and false alarm probability increases monotonously at the same time. The varying trends indicate that the performance

Table 1 Numerical results corresponding to different images in the field of view

Images	Fig. 3(a)	Fig. 3(b)	Fig. 3(c)	Fig. 3(d)	Fig. 3(e)	Fig. 3(f)
SA	0.451	0.447	0.415	0.408	0.379	0.312
P_{fa}	0.017 3	0.015 6	0.021 8	0.022 5	0.029 7	0.045 5
ESM(10^5)	2.03	2.11	2.16	2.25	2.40	2.49

Table 2 Numerical results corresponding to different images out the field of view

Images	Fig. 4(a)	Fig. 4(b)	Fig. 4(c)	Fig. 4(d)	Fig. 4(e)	Fig. 4(f)
SA	0.449	0.446	0.411	0.416	0.326	0.339
P_{fa}	0.011 9	0.014 3	0.027 1	0.022 6	0.052 6	0.128 4
ESM	283.5	289.7	311.1	327.1	334.7	340.1

However, the proposed ESM acquires more stabilized and effective results in evaluating the performance of laser jamming on CCD imaging detection systems even in complex EO scenes.

2.2 Performance comparison

In order to verify the feasibility of ESM metrics, the Search_2 dataset^[7-8] which is created by the TNO Human Factors Research Institute in the Netherlands is used to test our newly proposed metrics. Other two most widely used metrics, the Statistical Variance (SV) metrics^[11] and the Probability of Edge (POE) metrics^[12], and a effectively recently proposed Target Structural Similarity Metric (TSSIM)^[13] are used in the verification.



Fig. 5 The 5th image and it's full-size target scene from the Search_2 dataset

We use 39 original Search_2 images with only one search target and convert them into grayscale in the

of CCD imaging detection algorithms decreases obviously under the condition of laser irradiation. Meanwhile, the computed ESM increases monotonously along with incident laser power increasing, which could be used for the evaluation of laser interference performance on CCD detection algorithms.

What interests us is that the varying trends of computed SA and P_{fa} in Table 2 isn't consistent with that of Table 1, i. e., there are existing several irregular numerical values in the table, which indicates that the performance of CCD detection algorithms would become invalid when the incident laser power is high enough leading to a complex EO scene with serious laser interference.

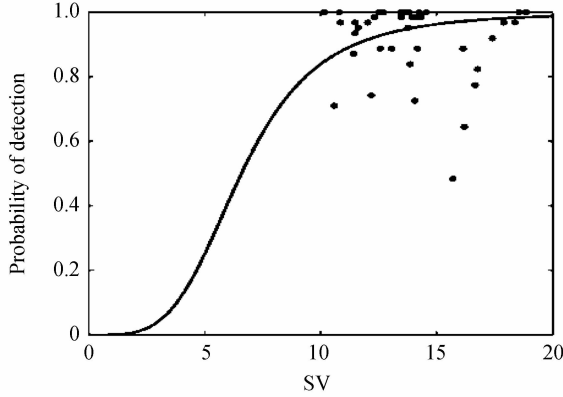
computation. The different image metrics values and detection probability in the Search_2 dataset are showed in Table 3.

Table 3 The different image metrics values, detection probability(PD) of each image in the Search_2 dataset

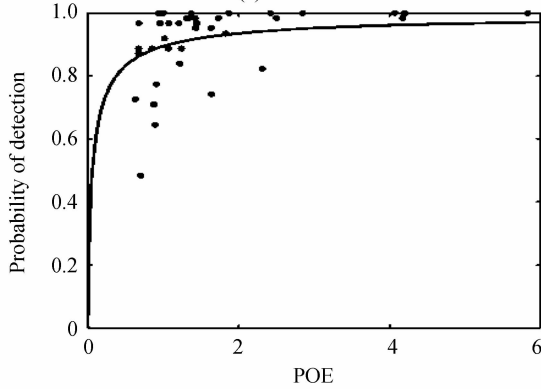
IMG_NO.	SV	POE	TSSIM	ESM	PD
1	13.862 4	122 000	0.124 3	1 084.9	0.839
2	12.189 3	163 760	0.213 5	1 783.8	0.742
3	14.174 4	124 050	0.141 3	1078.2	0.887
4	15.699 3	70 083	0.194 5	306.87	0.484
5	14.558 9	406 730	0.181 0	49 542	1
6	18.552 6	93 774	0.1933	671.27	1
8	16.136 8	85 052	0.158 5	625.2	0.887
9	14.238 4	582 560	0.100 4	45 001	1
10	14.324	173 110	0.166 6	2 472	0.984
11	10.583 3	87 451	0.209 9	1 020.6	0.71
12	10.149	186 870	0.157 1	12 492	1
13	12.498 8	137 000	0.132 5	2 249.7	1
14	11.488 5	182 600	0.130 9	6 157.2	0.935
16	13.953 7	133 890	0.145 4	2 155.8	0.984
17	10.813 0	96 016	0.174 2	1 851.8	1
18	13.484 4	142 120	0.105 6	4 491	0.984
19	16.770 9	231 280	0.135 9	9 149.4	0.823
20	11.617 8	163 480	0.186 6	6 951.2	0.952
21	16.659 8	90 853	0.157 5	824.88	0.774
22	16.193 5	89 547	0.241 3	853.911	0.645
24	11.422 1	67 253	0.124 6	616.333	0.871

25	12.034 9	95 571	0.197 9	1 240.5	0.968
27	12.566 3	106 920	0.185 5	1 000.6	0.887
28	13.675 5	136 860	0.117 2	2 821.7	1
29	13.067 6	67 166	0.117 4	226.632	0.887
30	17.901 8	107 240	0.156 5	1 082.2	0.968
31	12.715 9	242 050	0.144 4	9 808.5	1
32	14.072 6	63 294	0.210 7	366.635	0.726
33	11.49	67 399	0.094 2	1 233	0.968
34	14.272 2	417 120	0.140 0	76 222	0.984
35	18.861	419 620	0.177 1	35 692	1
36	10.856 7	120 480	0.146 2	3 952.3	0.968
37	14.073 2	250 050	0.197 8	14 409	0.984
38	13.764 6	142 670	0.197 3	5 150.2	0.952
40	12.304 6	130 860	0.101 5	6 432.7	0.984
41	13.796 1	284 380	0.133 3	22 654	1
42	13.450 3	100 180	0.124 4	2 234	1
43	18.382 6	144 180	0.129 2	2 772	0.968
44	17.416 2	101 580	0.123 6	483.9	0.919

In order to combine the metrics value with



(a) PD versus SV



(c) PD versus POE/($\times 10^5$)

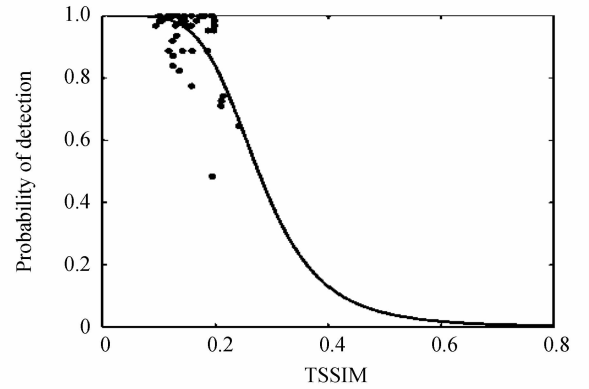
probability of detection in EO imaging systems, the following equation^[2] is adopted,

$$PD_{\text{pred}} = \frac{(X/X_{50})^E}{1 + (X/X_{50})^E} \quad (9)$$

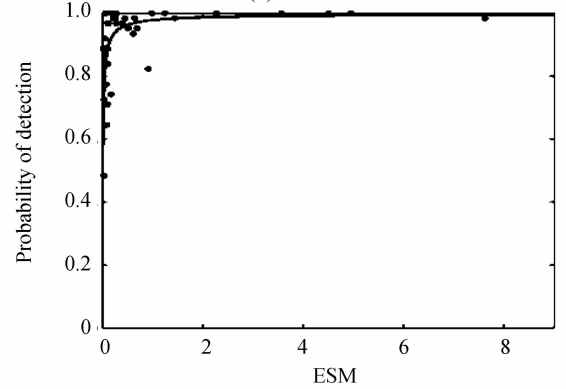
where is the Predicted Probability of Detection(PD), X is the predictor used in the prediction (ESM, SV, POE, TSSIM metrics value in this paper), E and X_{50} , the value of X for 50% detection, are determined by nonlinear regression.

The RMSE, Pearson correlation coefficient and Spearman correlation coefficient are employed to value the extent of the agreement between the detection probabilities predicted by the metrics and subjective experimental data. The fitting curves of detection probability versus the evaluated metrics value are shown in Figs. 6.

Each sample point stands for one test image in the Search_2 dataset. The computation results as well as the nonlinear regression parameters are listed in Table 4.



(b) PD versus TSSIM



(d) PD versus ESM/($\times 10^4$)

Fig. 6 Scatter plots of experimental target PD versus metrics values

Table 4 Performance comparison between different metrics

Metrics	X_{50}	E	RMSE	PCC	SCC
SV	-5.69	3.94	0.128	0.11	0.065
TSSIM	0.276	-5.09	0.098	0.556	0.341
POE	6 294.6	0.773	0.105	0.495 6	0.533 4
ESM	74.33	0.772	0.093	0.606	0.644

In the Table 4, E and X_{50} are curve-fitting

parameters, and RMSE is Root Mean Square(RMS) error. PCC^[14] represents Pearson correlation coefficient, and SCC^[15] is Spearman correlation coefficient. It is showed that the proposed ESM metrics has acquired the lowest RMS error and also, it has the highest PCC and SCC value, which has indicated that the ESM metrics is superior to SV, POE and TSSIM

metrics in the prediction of detection probability.

All the algorithms are computed on the software platform of MATLAB 2012a.

3 Conclusion

A laser jamming image metrics based on edge strength is proposed in this paper, which exploits the similarity between target image and subset block divided from laser jamming images for performance evaluation. The experimental results indicate that the ESM metrics is valid in describing laser interference on CCD imaging detection algorithms and its prediction correlates well with detection probabilities of observers in EO imaging systems. The method are suitable for the images with single target in and without serious background interference.

References

- [1] WANG Z, BOVIK A C, SHEIKH H R, *et al.* Image quality assessment: From error visibility to structural similarity[J]. *IEEE Trans on Image Process*, 2004, **13**(4): 600-612.
- [2] WILSON D L. Image-based contrast-to-Clutter modeling of detection[J]. *Optical Engineering*, 2001, **40**(4): 1852-1857.
- [3] XU Yin, SUN Xiao-quan, SHAO Li. Impact of laser jamming on target detection performance in CCD imaging system[J]. *Infrared Laser Engineering*, 2012, **41**(4): 899-993.
- [4] LI Qian, ZHANG Jian-qi, YANG Cui. Structure of the edge background clutter metric[J]. *Journal of Xidian University*, 2012, **39**(3): 95-96.
- [5] ZHANG Xuan-de, FENG Xiang-Chu, WANG WEI-wei, *et al.* Edge strength similarity for image quality assessment[J]. *IEEE Signal Processing Letters*, 2013, **20**(4): 319
- [6] XYDEAS C S, PETROVIC V. Objective image fusion performance measure[J]. *Electronics Letters*, 2000, **36**(4): 308-309.
- [7] TOET A, BIJL P, KOOI F L, *et al.* A high-resolution image data set for testing search and detection models[R]. TNO Human Factors Research Institute, 1998.
- [8] TOET A. Errata in report TNO-TM 1998-A020: A high-resolution image data set for testing search and detection models[R]. TNO Human Factors Research Institute, 2001.
- [9] LI MIN, ZHOU Zhen-hua, ZHANG Gui-lin. Image measures in the evaluation of ATR algorithm performance[J]. *Infrared and Laser Engineering*, 2007, **36**(3): 412-416.
- [10] ZHANG Ya-nan, TANG Xin-yi. Research on performance evaluation approaches of infrared automatic target recognition algorithms[J]. *Infrared*, 2007, **28**(6): 15-20.
- [11] SCHMIEDER D E, WEATHERSBY M R. Detection performance in clutter with variable resolution[J]. *IEEE Transactions on Aerospace and Electronic Systems*, 1983, **AES-19**(4): 622-630.
- [12] TIDHAR G, REITER G, AVITAL Z, *et al.* Modeling human search and target acquisition performance: IV. Detection probability in the cluttered environment [J]. *Optical Engineering*, 1994, **33**(3): 801-808.
- [13] CHANG Hong-hua, ZHANG Jian-qi. New metrics for clutter affecting human target acquisition [J]. *IEEE Transactions on Aerospace and Electronics System*, 2006, **42**(1): 361-368.
- [14] FIGUEIREDO M, NOWAK R, WRIGHT S. Gradient projection for sparse reconstruction: Application to compressed sensing and other inverse problems[J]. *IEEE Journal of Selected Topics in Signal Processing*, 2007, **1**(4): 586-597.
- [15] XU De-jiang, SHI Ze-lin, Luo Hai-bo. A structural different based image clutter metric with brain cognitive model constraints[J]. *Infrared Physics&Technology*, 2013, **57**: 28-35.